

A numerical study of planar arrays of correlated spin islands

I. Maccari¹, A. Maiorano^{1,2}, E. Marinari³, and J. J. Ruiz-Lorenzo^{4,2}

¹ Dipartimento di Fisica, Sapienza Università di Roma, P. A. Moro 2, 00185 Roma, Italy

² Instituto de Biocomputación y Física de Sistemas Complejos (BIFI) 50018 Zaragoza, Spain

³ Dipartimento di Fisica, IPCF-CNR and INFN, Sapienza Università di Roma, P. A. Moro 2, 00185 Roma, Italy

⁴ Departamento de Física and Instituto de Computación Científica Avanzada (ICCAEx), Universidad de Extremadura, 06071 Badajoz, Spain

April 12, 2016

Abstract. We analyze a system of interacting islands of XY spins on a triangular lattice. This model has been introduced a few years ago by Eley et al. to account for the phenomenology in experiments on tunable arrays of proximity coupled long superconductor-normal metal-superconductor junctions. The main features of the model are the separation of a local and a global interaction energy scale and the mesoscopic character of the spin islands. Upon lowering the temperature the model undergoes two crossovers corresponding to an increasing phase coherence on a single island and to the onset of global coherence across the array; the latter is a thermodynamical phase transition in the Ising universality class. The dependence of the second transition on the island edge-to-edge spacing is related to the proximity-effect of the coupling constant.

1 Introduction

Recently Eley et al. [1] have introduced a model of coupled islands of XY spins. Their goal was explaining the results of measurements of resistance in arrays of long superconducting-normal-superconducting junctions. The experimental devices are based on planar arrays of identical islands made of superconducting (Nb) grains, disposed in a triangular matrix over a metal (Au) film. The authors studied the dependence of the system resistance $R(T; h, \ell)$ on temperature T , on island (vertical) thickness h and on inter-island spacing ℓ . They found i) the resistance dropping to zero, by lowering T , in two steps, and they determined two transition temperatures T_1 and T_2 with $T_1 > T_2$; ii) an interesting dependence of both T_1 and T_2 on the island spacing, possibly (both) extrapolating to $T = 0$ at large ℓ ; iii) a strong dependence of the behavior of the system on the island thickness. In a following paper [2], they discussed a more detailed comparison between the experimental data and the predictions about the dependence of T_2 on ℓ given by the conventional theory of Lobb, Abraham, and Tinkham (LAT) [3]. They argued that for large inter-island spacing the superconducting transition is more likely to be driven by diffusive effects [4,5] in the normal metal substrate, and that it does not depend on the details of the superconducting islands, with the puzzling dependence on island height as a notable exception.

The superconducting transition in proximity-coupled *macroscopic* grains embedded in normal metal films has been the object of intensive work in the past years, [6,7,

8]. Tunable realizations of 2D superconductivity were also object of previous experiments [9]. The classical model presented in Ref. [1] to account for a novel phenomenology is at difference with previous theoretical and experimental work, as it takes into account the intrinsic fluctuations of the superconducting state inside the single *mesoscopic* islands (see also refs. [10,11] for recent theoretical and experimental work on mesoscopic Sn islands laid on graphene). It is clear that, because of many reasons we will discuss in the following, this model does not try to reproduce faithfully the experimental situation (for example the use of an anisotropic coupling is not connected to the physical form of the Josephson interaction but is a tool needed to obtain a phase transition). The idea of [1], and our point of view here, is to analyze a very simple model that offers a behavior quite similar to the one detected in the experiments, and to try to learn from this behavior. Here we will present a detailed analysis of the model, that corroborates and supplements the hints coming from the first analysis of [1]. It is also worth mentioning that tunable two-dimensional superconductors are also of interest in a revived search for a non-conventional 2D, $T = 0$ metallic phase. [12,13,14,15,16,17,18,19]

2 The model

The Hamiltonian of the model is based on $O(2)$ vectors living on the individual grains (labeled with i, j). Groups

of grains form islands (labeled by p):

$$H = -J \sum_p \sum_{\langle ij \rangle \in p} \mathbf{S}_i \cdot \mathbf{S}_j - \sum_{\langle p, p' \rangle} \mathbf{M}_p \cdot \mathbf{J}' \mathbf{M}_{p'}, \quad (1)$$

$$\mathbf{M}_p \equiv \sum_{i \in p} \mathbf{S}_i, \quad (2)$$

where by a dot we denote the scalar product in the internal space and where \mathbf{J}' is a 2×2 matrix of couplings. Each island is a D -dimensional hyper-cubic array of grains of linear size I (and volume $V_I = I^D$, with either $D = 1$ or $D = 2$ in our computations). Islands are arranged on a (two dimensional) planar regular lattice of linear size L . Islands are mesoscopic: their linear size I is not larger than a few grains. Because of that they may have large global phase fluctuations. The size of the underlying planar array is macroscopic, $L \gg I$. The case of one-dimensional island is an exercise useful to understand better the role of island dimensionality, and does not try to be a description of the experimental situation. On the contrary the case of two dimensional islands is probably closer to the experimental situation, where islands have many layers, but only one or few conjoin to build the inter-island interaction.

The first term of the Hamiltonian is a sum of nearest-neighbor interactions between grains contained in the same island. The second term couples neighboring islands in the array. Each spin in a given island interacts directly with its neighboring spins in the same island and with the average spin field of surrounding islands. In the model proposed in Ref. [1] the inter-island coupling matrix (in the internal $O(2)$ space) \mathbf{J}' is anisotropic:

$$\mathbf{J}' = \begin{pmatrix} J' & 0 \\ 0 & 0 \end{pmatrix}. \quad (3)$$

This particular choice polarizes the islands in one specific direction in internal vector space, changing the nature of the inter-island phase transition. This is a technically useful choice (since it carries a phase transition in the game), but it does not aim at reproducing the details of the physical Josephson interaction. Finally, notice that in the isotropic case and *if the energy scales J and J' are far apart, i.e. $J' \ll J$* , so that at low temperatures all (mesoscopic) islands are magnetized, we recover a Kosterlitz-Thouless [20] phase transition.

The island-island couplings depend on the temperature and on the inter-island edge-to-edge spacing, according to the theory of diffusion of electron pairs in SC-Normal-SC junction. As in the work of [1] we take a “quasi-proximity-effect” [1,3] form for both couplings; in a proximity interaction \mathbf{J}' would depend on the inverse square of island spacing when the latter is small, but following [1] and for the same sake of simplicity we omit this part of the interaction, that is not expected to change the nature of the phase transitions here. We assume the proximity-effect form also for the grain-grain coupling J and we take the

grain-grain distance as the length (lattice) unit (and denote the inter-island spacing as ℓ).

$$J = J_0 \exp(-\sqrt{T}), \quad (4)$$

$$\mathbf{J}' = \mathbf{J}'_0 \exp(-\ell\sqrt{T}). \quad (5)$$

The choice of an interaction of a proximity-like form implies that physically grains of the islands are also immersed into a metallic matrix. The authors of Ref. [1] introduced the model defined in (1) to explain the presence of two transitions (intra-island, T_1 , and inter-island coherence, T_2) and the depression of T_1 for increasing island spacing ℓ . Such a dependence of T_1 on ℓ has been observed and reported for the first time in [1] (for example in previous experiments on lead disks on a thin substrate [9] where islands were not mesoscopic, the effect was not observed). The energy scales J_0 and J'_0 must be well-separated: we adjust them in order to clearly split the high- T and the low- T transition. We fix $J_0 = 1$ and vary J'_0 ; in order to easily compare data for different island sizes, we also take $J'_0 = j'_0/V_I$ and adjust the parameter j'_0 .

In Ref. [1] the authors also give some predictions by analyzing a $D = 1$ islands model, where it turns out that:

- $T_2 \leq T_1$ provided $J \gg J'$ and islands are small;
- $T_1 \rightarrow 0$ when $J' \rightarrow 0$.

The second statement is rather counter-intuitive, as it implies that islands are not superconducting when they are isolated. This implies that an array of superconducting islands can be superconducting even if the inter-island spacing is larger than the superconductor coherence length, but an isolated island of superconducting grains, where grains are packed closer than islands are in the array, loses phase coherence. In this respect, the one-dimensional and mesoscopic character of the islands plays a role, since for macroscopic chains we must expect $T_1 \sim 0$, and, as we will see in the following, for large I the intra-island coherence is driven by inter-island ordering (also see the discussion in the Conclusions section).

Another striking aspect of the phenomenology of the system[1,2] is the dependence of its behavior from the height of columnar grains. Realistic islands extend in more than one dimension. We have analyzed by numerical simulations the behavior of one and two-dimensional islands. The dependence on thickness may suggest that it would be interesting to go to $D = 3$, too (in case of a very large value of I this should turn the T_1 transition to a true second-order one). If energy scales are adequately separated (i.e. $J \gg J'$), this should not change the properties of the T_2 (KT) transition, when phases of grains in the same island are mutually locked. Mesoscopic islands can then have a crossover at T_1 from a disordered to an ordered phase; for $D \geq 2$ and large I this crossover is related to a true thermodynamic transition.

3 Numerical simulations

We have studied the model defined in (1). By following a very slow annealing protocol, with constant ratios between

adjacent temperature (a logarithmic annealing scale), we have cooled down the system in order to get a signal for the two transitions. At each temperature we collected measurements during the evolution of the Monte Carlo dynamics. Our Monte Carlo step consists of n_m sweeps of the whole lattice by single-spin moves Metropolis dynamics, followed by n_o sweeps by over-relaxation [22]. The choice of $n_m = 10$ and $n_o = 12$ have shown to be appropriate for most island and array sizes considered (and an overkill for the smaller sizes), and allowed an estimate of integrated auto-correlation times not larger than ten Monte Carlo steps at most temperatures. Although averages always stabilize quickly after any temperature change, we drop the first half of the collected measurements at all T values. The simulated annealing protocol, together with over-relaxation, is appropriate to the needs of this problem. All observables of interest converge very fast to a plateau at all temperatures. Although averages always stabilize quickly after any temperature change, we drop the first half of the collected measurements at all T values.

Since the devices in the experimental setup [1, 2] are triangular arrays, we consider a triangular lattice. A sim-

ple implementation choice in simulation is to consider a triangular array with regular hexagonal shape with helical boundary condition (in this way we preserve the symmetries of the triangular array and avoid involved bulk properties extrapolations); each side of the hexagon has a width of L islands, and the number of islands is $V_S = 3L(L-1) + 1$. We simulated systems with $L = 8, 16$ and 32 : for $D = 1$ systems we have islands of sizes $I = 16, 36, 64, 100$ and 144 , while for $D = 2$ we have $I = 6, 8, 10$ and 12 . The inter-island edge-to-edge spacing ℓ has been varied in the set $\{2, 4, 8, 12\}$ for $D = 1$ and $\{2, 4, 8, 12, 16, 24\}$ for $D = 2$ (the SNS arrays in Ref. [1] had edge-to-edge spacings up to approximately 10 times the grain size in their experiments, and ℓ up to 20 in Ref. [2]). We have considered both free (FBC) and periodic (PBC) boundary conditions on the single islands. Although we found no qualitative differences, FBC is a more realistic choice when dealing with mesoscopic objects, for which we expect finite-size effects to play a role. We measured the following quantities.

- The *single island magnetization magnitude* (averaged over islands):

$$M_I = \frac{1}{V_S} \sum_p \left| \frac{1}{V_I} \sum_{i \in p} \mathbf{S}_i \right|. \quad (6)$$

This should be, in the limit of infinitely extended islands, a good order parameter for island internal ordering (in any direction in internal spin space, and globally over the array: it has a non-zero value whenever any island starts to order internally and it is maximum when all islands are locally ordered, independently of the relative orientation between different islands).

- The total magnetization:

$$\mathbf{M} = \frac{1}{V_S V_I} \sum_p \sum_{i \in p} \mathbf{S}_i. \quad (7)$$

- A renormalized magnetization:

$$\boldsymbol{\mu}_p = \frac{\sum_{i \in p} \mathbf{S}_i}{\left| \sum_{i \in p} \mathbf{S}_i \right|}, \quad (8)$$

which is a unit vector on the single island, and its average over the array.

- M_R , which characterizes the globally-ordered phase, even if islands are not yet internally fully ordered:

$$M_R = \frac{1}{V_S} \sum_p \boldsymbol{\mu}_p. \quad (9)$$

We also consider the fluctuations of the magnetizations

$$\chi \equiv V_I V_S \left[\langle M^2 \rangle - \langle |M| \rangle^2 \right], \quad (10)$$

$$\chi_I \equiv V_I \left[\langle M_I^2 \rangle - \langle M_I \rangle^2 \right], \quad (11)$$

$$\chi_R \equiv V_S \left[\langle M_R^2 \rangle - \langle M_R \rangle^2 \right], \quad (12)$$

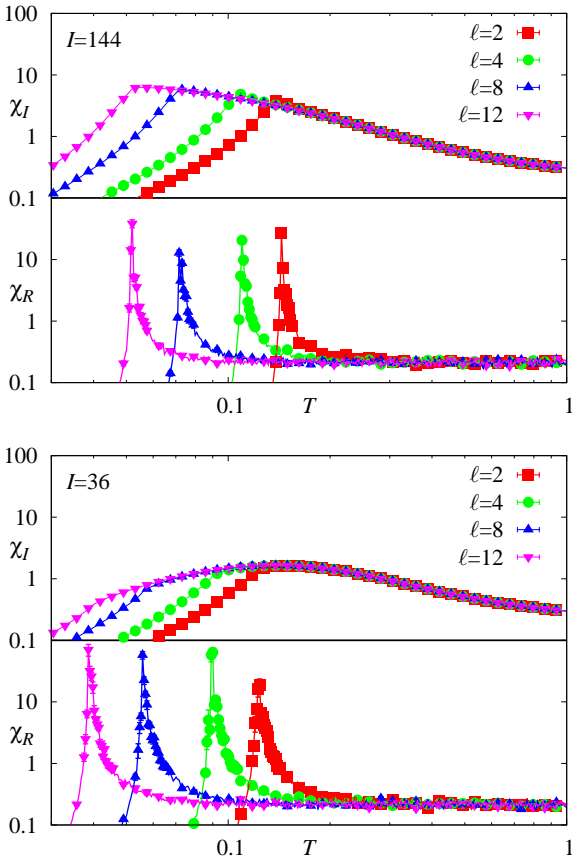


Fig. 1. $D = 1$ results for the largest simulated size $L = 32$. We plot the connected susceptibilities χ_I and χ_R for two different values of I . $j'_0 = 0.0072$. On each panel we also plot the curves for four values of the island spacing ℓ . Notice that the peaks of χ_I (which mark the T_1 transition) depend strongly on ℓ .

where $\langle M_I^2 \rangle$ and $\langle M_I \rangle$ are averaged over all islands. χ is the total susceptibility of the system. At very low temperatures, when $M_I \sim 1$, we have $\chi_R \sim \chi/V_I$. At T_2 , that we define as the location of the peak of the inter-island susceptibility χ_R , χ_R and χ have very similar sharp peaks (both in shape and location). We take the location of the (very smooth) maximum of χ_I as a rough estimate of the temperature T_1 at which islands order internally (in this way we give an operative definition of T_1 in our model: since islands are of finite extent the T_1 defined in this way is indeed a crossover temperature).

4 Results and discussion

In Fig. 1 we report the results for arrays of one-dimensional chains. The T_1 temperature value goes to zero very fast as the island size grows, as expected for linear spin chains. Upon lowering T , coherence between island builds up and also drives the internal ordering; the two transitions can be resolved only for very small island sizes and by lowering considerably the value of coupling constant j'_0 . The effect is also strongly dependent on island size.

The situation is far clearer for two-dimensional islands (see Fig. 2), where we still have a finite temperature thermodynamic transition for isolated islands in the limit of large sizes. For mesoscopic islands, the crossover between unordered and ordered island depends more weakly on island size than in the linear chains case. Our numerical simulations show that the temperature T_1 does not depend on the island spacing, or the dependence is very weak. This effect has been also reported in experimental results on non-mesoscopic island samples [9]. Also the dependence of T_1 on island size is very weak.

We try a more quantitative approach studying the depression of T_2 by increasing the inter-island spacing. We take as an estimate for T_2 the midpoint of the temperature interval bracketing the peak at its half-height. The dependence of T_2 on ℓ and I for the largest simulated array size $L = 32$ is shown in Fig. 3.

Following Ref. [1], we notice that $T_2(\ell)$ compares well to a proximity-effect prediction

$$T_2 = \Delta \exp(-C\ell\sqrt{T_2}), \quad (13)$$

corresponding to the solid straight line in Fig. 3, suggesting a diverging $\ell(T_2 = 0)$; we report in Table 1 our best fit estimates of the parameters Δ and C .

We have run more accurate numerical simulations in the temperature region close to the T_2 transitions, with a four times smaller cooling rate and ten times more measurements. We measured the Binder cumulant

$$G_4 = \frac{1}{2} \left(3 - \frac{\langle (M^2)^2 \rangle}{\langle M^2 \rangle^2} \right). \quad (14)$$

The value of G_4 at the T_2 transition point is universal [22]; we report data for $I = 6$, $\ell = 4$ and various array sizes L in Fig. 4. Note that the dips in the curves of G_4 for the

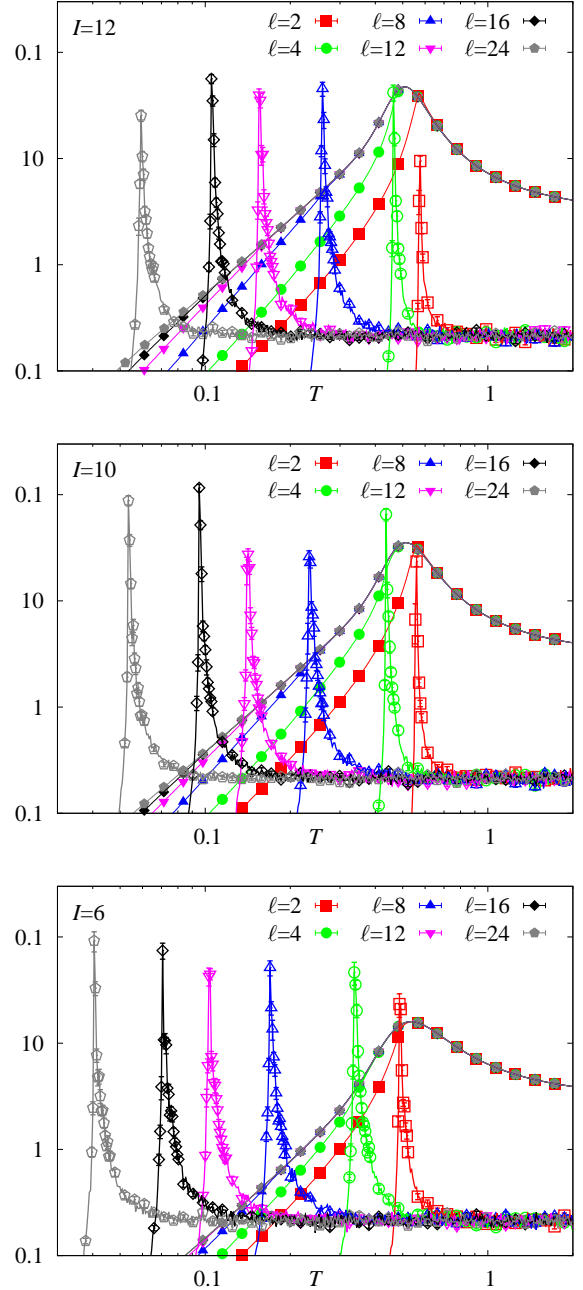


Fig. 2. $D = 2$ results for the largest simulated size $L = 32$. We plot the connected susceptibilities χ_I (filled symbols) and χ_R (empty symbols) for three different pairs of the parameters I and j'_0 . On each panel we plot the curves for six values of the island spacing ℓ . The peaks of χ_I (which mark the T_1 transition) depend only weakly on ℓ . In all panels $j'_0 = 0.072$

largest system sizes in Fig. 4 are due to the breakdown of the $O(2)$ internal symmetry introduced by the anisotropic form of J' in Eq. (3). This is the behavior one would expect, since at high temperature the G_4 value depends on the symmetry of the system. The fluctuations of the magnetization in the infinite volume limit are Gaussian dis-

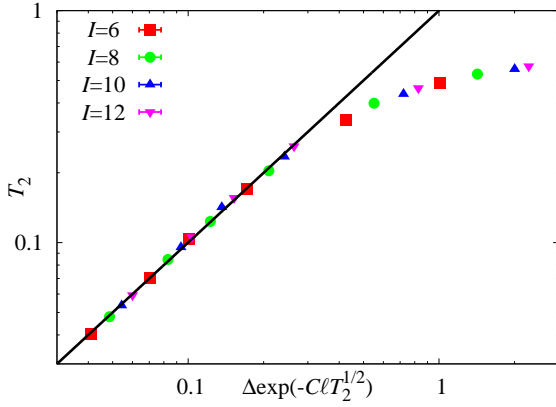


Fig. 3. A scaling plot of the T_2 transition temperature for arrays of $D=2$ island based on the behavior $\Delta \exp(-C\ell T_2^{1/2})$ as suggested by Eq. 5 ($L = 32$ data).

tributed and the Binder parameter for the two-component magnetization of a XY system should approach the value $G_4(T \rightarrow \infty) = 0.5$, whereas for Ising spins the corresponding high-temperature value is $G_4(T \rightarrow \infty) = 0$. When long range order in the system builds up at low temperatures, the value of the Binder parameter must approach unity: $G_4(T \rightarrow 0) = 1$. The data in Fig. 4 show that G_4 is not monotonically increasing when the temperature decreases: it starts at a value around 0.5 but, as soon as the inter-island term becomes more important with respect to the intra-island interaction in the Hamiltonian, the effects of the Ising symmetry sets in and in proximity of the critical region, just above T_2 , the value of G_4 drops to low values, as expected for an Ising system. The minimum of the dip decreases as the system size L increases.

Moreover, the critical value of the Binder cumulant (which is universal) for the two-dimensional Ising model is known to great accuracy [23]. The values $G_4 = 0.9160386(24)$ compares extremely well with our value of the Binder parameter at crossing, close to $T_2 \sim 0.335$ (for comparison, from the position and width at half-height of the peak of the susceptibility for the same simulated system we obtain $T_2 \simeq 0.340 \pm 0.004$). We report in Fig. 5 the details of the crossing of the Binder curves. This provides a clear

I	Δ	C
6	3.74(10)	0.935(6)
8	5.21(15)	0.890(6)
10	7.56(28)	0.889(7)
12	8.15(26)	0.840(6)

Table 1. Best fit estimates of Δ , C parameters in Eq. 5 from T_2 data for various island size I ($D = 2$, $L = 32$, $\ell = 8, 12, 16, 24$). Data points for the shortest distances $\ell = 2, 4$ have been excluded from the fits. The chi-square per degree-of-freedom values vary between 2.4 and 3.7 and the quality-of-fit parameters between 0.11 and 0.32. Uncertainties are gnuplot estimates corrected as in [21].

numerical evidence for a second order phase transition in the two-dimensional Ising universality class. The asymptotic value of the crossing points of the Binder cumulants curves (see inset of Fig. 5), $T_{2c}(L, 2L)$ which asymptotically tends to T_2 , is clearly different from zero. We finally remark that the value of the Binder cumulant below the critical temperature is almost unity as expected asymptotically (as the size of the system goes to infinity).

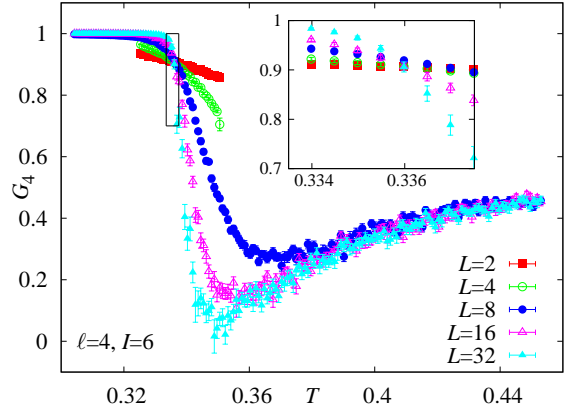


Fig. 4. Binder cumulant G_4 versus T for $D = 2$ -islands with $I = 6$ and $\ell = 4$ and for the five simulated sizes (L). In the inset we show in detail the region near $T \sim 0.335$, where different Binder curves cross.

5 Conclusions

It has been very difficult to resolve the crossover at T_1 (internal island ordering) and the T_2 transition (inter-island ordering) in the case of one-dimensional islands. In $D = 1$ and in the limit of large islands sizes we expect $T_1 \rightarrow 0$ and no thermodynamic transition at finite temperatures. In the range of simulated island sizes the measured crossover temperature at which the mesoscopic island order internally is as small as T_2 . The island internal magnetization remains small and no clear maximum of the susceptibilities signals a crossover down to T_2 . At T_2 the inter-island interaction couples the fluctuations of the magnetizations of neighboring islands, making them coherent: at this point spins inside each islands starts to align to the average field of neighboring islands. The mesoscopic character of the islands is crucial: in the limit of large islands we expect the fluctuations of local magnetization to be too small (we did not try an experiment in that direction). Then, although $J' \ll J$, it is the T_2 transition that drives both inter-island and internal ordering. As the inter-island spacing grows the depression of T_2 implies the depression of T_1 , too. This is compatible with the counterintuitive requisite that $T_1 \rightarrow 0$ as $J' \rightarrow 0$ discussed above.

Since islands in experimental setups are not laid down on the substrate as unidimensional chains of columnar

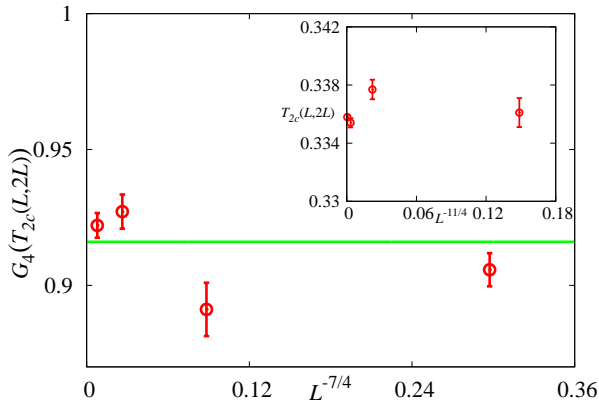


Fig. 5. Binder cumulant $G_4(T_{2c}(L, 2L))$, for $D = 2$ -islands with $I = 6$ and $\ell = 4$, computed at the crossing point of the Binder curves of lattice sizes L and $2L$, denoted as $T_{2c}(L, 2L)$, as a function of $L^{-7/4}$. We have marked, with a green horizontal line, the G_4 value for the two dimensional Ising model: $G_4 = 0.9160386$. In the inset we show the behavior of the temperature-value of the crossing point $T_{2c}(L, 2L)$ of the Binder curves as a function of $L^{-11/4}$. We have assumed the scaling of the two dimensional Ising model: $T_{2c}(L, 2L) - T_2 \sim L^{-\Delta-1/\nu}$ and $G_4(T_{2c}(L, 2L)) - G_4(T_2) \sim L^{-\Delta}$. We have used the exact value $\nu = 1$ and the conjectured one for the correction-to-scaling exponent $\Delta = 7/4$. For more details, see Ref. [23].

grains, the 1D system is not really connected to the experimental setup we analyze here. The 2D island system is, on the contrary, closer to the physical system we want to understand, and resolving the two transitions is easier in the case of the $D = 2$ system. The T_1 transition for $D = 2$ macroscopic islands and for $J' \ll J$ is expected to be of the Kosterlitz-Thouless type. Since we consider mesoscopic, finite islands, we observe, as expected, a “long-range” ordering of the islands. We expect a spin ordering crossover at a temperature value T_1 which does not go to zero with the island size as fast as in the $D = 1$ case. The model with planar islands is capable of describing the depression of the global superconductivity transition down to very low temperature at large lattice spacing. The transition temperature we measure by locating the peaks of response functions remains finite for moderate-to-large inter-island edge-to-edge spacing. T_2 approaches a zero value only for very large inter-island spacing. We cannot detect any dependence of the T_1 transition temperature on ℓ . At small ℓ values, the value of T_1 is influenced by nearby islands only because of global coherence driving internal ordering. We did not try a full finite-size scaling analysis of the T_2 transition, which for well-separated coupling scales j_0 and j'_0 is in the Ising universality class. On the simulated length scales there are no relevant effects of the mesoscopic character of the islands on the behavior of T_2 , which behaves at large inter-island spacings as expected by the choice of the dependence of the coupling constants on ℓ and T .

Appropriate variations of the basic model we have discussed here could lead to interesting developments in the study of the superconducting transition in arrays of SNS junctions. We think it is an interesting starting point to understand many striking experimental evidences, as for instance the dependence of the transition temperatures on island thickness, or the strong depression of the T_1 and T_2 transitions.

We thank Kay Kirkpatrick for introducing us to the model studied in this work and her and Jack Weinstein for interesting discussions. This work was partially supported by European Union through Grant No. PIRSES-GA-2011-295302, and ERC Grant No. 247328, by the Ministerio de Ciencia y Tecnología (Spain) through Grant No. FIS2013-42840-P, and by the Junta de Extremadura (Spain) through Grant No. GRU10158 (partially founded by FEDER).

References

1. S. Eley, S. Gopalakrishnan, P.M. Goldbart and N. Mason, *Approaching zero-temperature metallic states in mesoscopic superconductor-normal-superconductor arrays*, Nat. Phys. **8**, 59 (2012).
2. S. Eley, S. Gopalakrishnan, P.M. Goldbart and N. Mason, *Dependence of global superconductivity on inter-island coupling in arrays of long SNS junctions*, J. Phys: Condens. Matter **25**, 445701 (2013).
3. C.J. Lobb, D.W. Abraham, M. Tinkham *Theoretical interpretation of resistive transition data from arrays of superconducting weak links*, Phys. Rev. **27** 150 (1983).
4. F.K. Wilhelm, A.D. Zaikin, Gerd Schön *Supercurrent in a mesoscopic proximity wire* J. Low Temp. Phys **106** 305 (1997).
5. P. Dubos, H. Courtois, B. Pannetier, F. K. Wilhelm, A. D. Zaikin and G. Schön, *Josephson critical current in a long mesoscopic S-N-S junction*, Phys. Rev. B **63** 064502 (2001).
6. B. Spivak, A. Zyuzin, and M. Hruska, *Quantum superconductor-metal transition*, Phys. Rev. B **64** 132502 (2001).
7. B. Spivak, P. Oretto, and S.A. Kivelson, *Quantum superconductor-metal transition*, Phys. Rev. B **77** 214523 (2008).
8. M.V. Feigel'man, A.I. Larkin, and M.A. Skvortsov, *Quantum Superconductor-Metal Transition in a Proximity Array*, Phys. Rev. Lett. **86** 1869 (2001).
9. D.J. Resnick, J.C. Garland, J.T. Boyd, S. Shoemaker and R.S. Newrock, *Kosterlitz-Thouless Transition in Proximity-Coupled Superconducting Arrays*, Phys. Rev. Lett. **47** 1542 (1981).
10. M.V. Feigel'man, M.A. Skvortsov and K.S. Tikhonov, *Proximity-induced superconductivity in graphene*, JETP Lett. **88**, 747 (2008).
11. B.M. Kessler, Ç.Ö. Girit, A. Zettl and V. Bouchiat, *Tunable Superconducting Phase Transition in Metal-Decorated Graphene Sheets*, Phys. Rev. Lett. **104**, 047001 (2010).
12. P. Phillips and D. Dalidovich, *The Elusive Bose Metal*, Science **302** 243 (2003).

13. A. Punnoose and M. Finkel'stein, *Metal-Insulator Transition in Disordered Two-Dimensional Electron Systems*, Science **310**, 289 (2005).
14. S.V. Kravchenko and M.P. Sarachik, *A metal-insulator transition in 2D: Established facts and open questions*, in *50 Years Of Anderson Localization*, ed. by E. Abrahams, 2010 World Scientific, Singapore.
15. S.V. Kravchenko and M.P. Sarachik, *Metal-insulator transition in two dimensional electron systems*, Rep. Prog. Phys. **67**, 1 (2003).
16. A. Shashkin and S.V. Kravchenko, *Quantum phase transitions in two-dimensional electron systems*, in *Understanding Quantum Phase Transitions*, ed. by Lincoln D. Carr, 2010 Taylor & Francis, Boca Raton.
17. J. Biscaras, N. Bergeal, C. Feuillet-Palma, A. Rastogi, R.C. Budhani, M. Grilli, S. Caprara, and J. Lesueur, *Multiple quantum criticality in a two-dimensionale superconductor*, Nat. Mater. **12**, 542 (2013).
18. Wei Liu, LiDong Pan, Jiajia Wen, Minsoo Kim, G. Sambandamurthy, and N.P. Armitage, *Microwave Spectroscopy Evidence of Superconducting Pairing in the Magnetic-Field-Induced Metallic State of InO_x Films at Zero Temperature*, Phys. Rev. Lett. **111**, 067003 (2013).
19. Zheng Han, A. Allain, H. Arjmandi-Tash, K. Tikhonov, M. Feigel'man, B. Sacépé and V. Bouchiat, *Collapse of superconductivity in a hybrid tin-graphene Josephson junction array*, Nat. Phys. **10**, 380 (2014).
20. J.M. Kosterlitz and D.J. Thouless, *J. Phys. C : Solid State Phys.* **6** 1181 (1973);
J.M. Kosterlitz, *J. Phys. C : Solid State Phys.* **7** 1046 (1974).
21. A.P. Young, *Everything you wanted to know about Data Analysis and Fitting but were afraid to ask*, (Springer, Berlin 2015), Appendix D.
22. D. Amit and V. Martin-Mayor, *Field Theory, the Renormalization Group, and Critical Phenomena: Graphs To Computers* (World Scientific, Singapore 2005).
23. A. Sokal and J. Salas, *Universal Amplitude Ratios in the Critical Two-Dimensional Ising Model on a Torus*, J. Stat. Phys. **98**, 551 (2000).